Journal of New Materials for Electrochemical Systems 5, 213-221 (2002)

Novel Electrochromic Batteries: II. An InHCF-WO_3 Cell with a High Visual Contrast

Lin-Chi Chen, Kuei-Sheng Tseng, Yu-Hsien Huang, and Kuo-Chuan Ho*

Department of Chemical Engineering
National Taiwan University
Taipei 10617, Taiwan

(Received June 21, 2001 ; received in revised form January 3, 2002)

Abstract: *Upon the improvements in the electrodeposition of indium hexacyanoferrate (InHCF) thin film, another novel thin-film electrochromic battery (ECB) based on InHCF and WO_3, namely IWECB, was proposed and investigated. By using the KCl-saturated poly-2-acrylamido-2-methylpropane sulfonic acid (K-PAMPS) electrolyte, an IWECB can be charged/discharged between 0.70 V and 1.70 V and features a theoretical voltage of ca. 1.24 V. Moreover, an IWECB exhibits blue-to-colorless electrochromism, with a coloration efficiency of ca. 46.0 cm^2/C at 650 nm during the discharging (bleaching) process; therefore, it offers a better visualization of the state of charge (SOC) than a Prussian blue-WO_3 ECB (PWECB) does. In addition, it was revealed that the IWECB with such a high visual contrast possesses a dual energy-saving function, in which an IWECB can act as a rechargeable battery and/or a solar-attenuated window. Accordingly, an IWECB-based window can be charged and colored by a photovoltaic (PV) cell in the daytime to store the solar energy and to attenuate solar irradiation in the meantime. This elucidates that an IWECB can greatly enhance the use of the solar energy. Besides the above advantages, the dynamic and at-rest stabilities of an IWECB are discussed in this paper.*

Key words : Coloration efficiency, electrochromic battery (ECB), indium hexacyanoferrate (InHCF), solar attenuation, tungsten oxide (WO_3).

1. INTRODUCTION

In our previous paper [1], the superior applicability of a thin-film electrochromic battery (ECB) based on Prussian blue (PB) and WO_3, namely PWECB, was revealed and demonstrated. In combination with the KCl-saturated poly-2-acrylamido-2-methylpropane sulfonic acid (K-PAMPS) electrolyte that accommodates the conduction of both K^+ and H^+, the rechargeable thin-film PWECB with a theoretical voltage of 1.35 V was able to drive an 8-digit electronic calculator for several hours; moreover, it was disclosed that by conjoining the ECB with a photovoltaic cell (PV), a PWECB achieves the goal of the all-solar-driven electronic device and provides an opportunity to reduce the consumption of primary button cells, which are harmful to our environment. Furthermore, the most promising advantage of an ECB is its electrochromic nature, which helps to visually quantify the residual charge. The visualization of the state of charge (SOC) can allow people to judge with the naked eye if a cell needs to be recharged. It was described previously that a PWECB shows dark green-to-blue electrochromism corresponding to the charge-to-discharge transition and thus offers visualization of the SOC; however, the visual contrast between the charged and discharged states is not high and becomes less distinguishable when the PWECB is assembled with high-capacity electrodes, which result in a deep, darker color. Therefore, to overcome this low contrast issue, an ECB with a high visual contrast is presented here. Indium hexacyanoferrate (InHCF) [2-6], which exhibits the yellowish-to-colorless

*To whom correspondence should be addressed: Fax: +886-2-2362-3040; Tel: +886-2-2366-0739; Email: kcho@ms.cc.ntu.edu.tw

electrochromism [4-6] and has a high redox potential of *ca.* 0.72 V *vs.* SCE [2-5], is assembled with WO_3, in conjunction with the K-PAMPS electrolyte to result in an InHCF-WO_3 ECB (IWECB).

InHCF is an analogue of PB (iron (III) hexacyanoferrate (II)) [7-8], which is an important class of mixed valence polynuclear compounds and provides a zeolitic lattice [9-10] for the cationic insertion/extraction during redox processes. Similar to PB, a "soluble-form" InHCF ($In[Fe(CN)_6]$, yellowish) film can reversibly be reduced to the colorless $KIn[Fe(CN)_6]$ (namely, KInHCF) accompanied by the insertion of K^+[2-6]. Being aware of the light, yellowish/colorless electrochromism, Spindler [11] disclosed that a complementary electrochromic device (ECD) using InHCF, a transparent counterelectrode, has the advantage of eliminating precoloration. Recently, we also developed a new complementary PB-InHCF ECD [12], in which the potential difference between the colored and bleached states could be as small as 0.4V. Besides, InHCF has been researched for applications in biosensors [13], photoelectrochemical converting material [14], and photoelectrode-stabilizing coating [15]. Although InHCF can be used in a variety of applications, the difficulty in preparing an InHCF film with a large capacity limits its applicability in batteries.

An InHCF film can be prepared by cyclic voltammetric (CV) electrodeposition [2-3], potentiostatic electrodeposition [4-5], or the sacrificial anode method [6]. No matter which approach is employed, the formation of an InHCF plating solution is similar to the typical recipe of a PB plating solution, which is an aqueous solution composed of equal-molar ferric and ferric cyanide ions (says, 10 mM) with indefinite amounts of K^+ and H^+. In other words, an InHCF plating solution contains equal concentrations of In^{3+} and $[Fe(CN)_6]^{3-}$. However, unlike the aqueous mixture of Fe^{3+} and $[Fe(CN)_6]^{3-}$, In^{3+} co-precipitates with $[Fe(CN)_6]^{3-}$ in a short time when both concentrations are higher than several mM, and an instability in the plating solution is therefore encountered. As a result, most of the InHCF plating solutions reported in literature employed a highly diluted aqueous mixture of In^{3+} and $[Fe(CN)_6]^{3-}$ (< 1 mM) [2-3, 16-17]. Apparently, the charge capacity of an InHCF film electrodeposited from a dilute plating solution would be too small for a battery. Similar problems were encountered in a low-voltage PB analogue (PBA)-based secondary battery [18]. Grabner *et al.* [18] reported that a thin-film secondary battery, based on copper hexacyanoferrate (CuHCF) and PB, possessed a charge capacity of only 3-9 mC/cm^2. Although a zinc hexacyanoferrate (ZnHCF)-PB battery with a practical capacity of 12 Ah/kg and a CuHCF-PB battery with a practical capacity of 5 Ah/kg were achieved by the PBA/graphite paste electrodes (non-thin-film electrodes) [19], the opaque graphite paste is extremely disadvantageous to electrochromism. Therefore, improving the electrodeposition of InHCF films is the best solution for the capacity issue.

Our recent work has revealed that the stability of an InHCF plating solution can be greatly improved by adding large amounts of H^+ and/or K^+ [20]. It was found that a fresh plating solution, containing only 10-mM In^{3+} and $[Fe(CN)_6]^{3-}$, becomes useless within couples of minutes, whereas the same plating solution with 1N HCl and 1N KCl added to it could be stored freshly for over a week. In addition, it was verified that adding H^+ prompts the electrodeposition of InHCF on the F-doped SnO_2 (FTO) glass electrode and increases the electrodeposited capacity by a factor of 18 ~19. Furthermore, InHCF films grown in a H^+-rich environment were found to be superior, as judged by their electrochemical behavior. On the basis of the above findings, an IWECB, using an InHCF film prepared in the improved plating solution by the CV electrodeposition, is investigated in this work. In this paper, an IWECB with a theoretical cell voltage of 1.24V, which is applicable to low-power electronic devices, is demonstrated. Moreover, it will be shown that an IWECB exhibits a high visual contrast between the charged (colorless) and discharged (blue) states. Such a high visual contrast not only enhances the visualization of the SOC but also allows the IWECB to act as a solar-attenuated window. As a consequence, in combination with a photovoltaic (PV) cell, an IWECB will lead to a better use of solar energy (stores solar energy as well as acting as a solar-attenuated window simultaneously). In addition to elucidating the above advantages of an IWECB, both the electrochromic and electrochemical characteristics will be presented and discussed later.

2. EXPERIMENTAL

In this work, most of the experimental conditions were the same as those reported in the previous PWECB work [1]. Hence, only the unique procedures are described as follows.

2.1 Preparation of the InHCF film and cell assembly

The InHCF film was deposited onto a clean FTO glass substrate (Sinonar, T_{550nm} = 80%, R_{sh} = 20 Ω/sq.) with an electroactive area of 3.0×1.5 cm^2, using the CV electrodeposition. According to the conclusions from the improvements on InHCF electrodeposition [20], a plating solution, composed of 10 mM $InCl_{3(aq)}$ and 10 mM $K_3Fe(CN)_{6(aq)}$ with the presence of 1 N KCl and 1 N HCl, was used. During electrodeposition, dynamic potential scanning back and forth between 0.2 V to 1.3 V (*vs.* Ag/AgCl/Sat'd KCl) at a rate of 0.2 V/s was applied to the FTO substrate for 30 cycles. After plating, the as-prepared InHCF film was washed with deionized water (DIW) and then dried in air for at least 24 hours before using. The thickness of an InHCF film was measured by a profile meter (Tencor, Alpha step-200).

For cell assembly, an as-prepared InHCF (the reduced form) electrode and a post-heated WO_3 electrode were used as the positive and negative electrodes, respectively. A fresh K-PAMPS electrolyte was sandwiched in between these two electrochromic

(EC) electrodes resulting in a laminated IWECB. The assembly was carried out in ambient conditions at room temperature. Similar to the PWECB system, WO_3 was not prepolarized to H_xWO_3 in advance. After assembling, the IWECB with an active area of 3.0×1.5 cm^2 was sealed with the Torr Seal cement (Varian, MA, USA).

2.2 Electrochemical characterizations of the electrochromic electrodes in K-PAMPS

The InHCF and WO_3 films were electrochemically characterized in K-PAMPS electrolytes [1], using a three-electrode CV, to estimate the formal potentials and redox capacities for the InHCF/KInHCF and WO_3/H_xWO_3 redox systems. The K-PAMPS electrolyte had an ionic conductivity of *ca.* 101 mS/cm at room temperature and had a molar ratio of H_2O to AMPS of *ca.* 7.2 [1]. When preparing the solid polymer electrolyte, KCl was chosen on purpose for two reasons. First, chloride ions are compatible with the saturated KCl used in a Ag/AgCl reference electrode. Secondly, when cycling the Prussian blue or its analogs, potassium ions are usually chosen and reported. Cyclic voltammetry was performed with a potentiostat/galvanostat (ECO-Chemie, Autolab, PGSTAT30); silver wire and platinum plate were used as the pseudo-reference and auxiliary electrodes, respectively. The pseudo-reference electrode was assumed to have a redox potential identical to the redox potential of an Ag/AgCl electrode immersed in a saturated KCl solution.

2.3 *In situ* spectroelectrochemical and electrochemical characterizations of IWECBs

For the *in situ* spectroelectrochemical characterizations, an IWECB was connected to the above-mentioned potentiostat/galvanostat and placed in a spectrophotometer (Shimadzu, model UV-1601PC) to collect the transmittive spectra at different equilibrated cell voltages. For the electrochemical characterizations, a multi-channel battery test system (Maccor, Model 2300) was employed to obtain the typical charge/discharge and self-discharging behaviors of an IWECB. When characterizing an IWECB, the cell voltage (InHCF *vs.* WO_3) was recorded. Additionally, the IWECB was photographed, at both cell voltages, 0.70 V and 1.70 V, to demonstrate the high visual contrast.

3. RESULTS AND DISCUSSION

3.1 An IWECB with a theoretical cell voltage of 1.24 V

3.1.1 Formal potentials of the InHCF and WO_3 electrodes in the K-PAMPS electrolyte

The typical CVs, for an as-prepared InHCF film with a thickness of 1.99 μm and a post-heated WO_3 film with a thickness of 0.45 μm in the K-PAMPS electrolyte, are shown in Fig. 1. Since it was demonstrated previously [1] that a K-PAMPS electrolyte accommodates the conduction of both K^+ and H^+, here it is considered that the InHCF and WO_3 electrodes immersed in the K-PAMPS electrolyte undergo the following redox reactions, as suggested in literature [2-6, 21-23]:

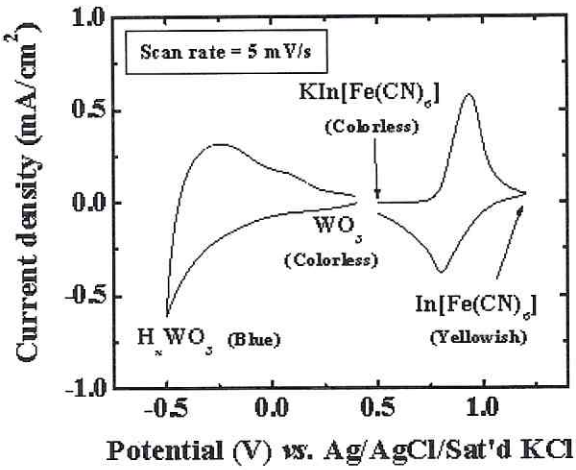

Figure 1: Typical cyclic voltammograms for the InHCF/KInHCF and WO_3/H_xWO_3 redox couples.

$$In[Fe(CN)_6] \text{ (yellowish)} + K^+ + e^- \leftrightarrow KIn[Fe(CN)_6] \text{ (colorless)} \quad (1)$$

$$WO_3 \text{ (colorless)} + x\ H^+ + x\ e^- \leftrightarrow H_xWO_3\text{(blue)} \quad (2)$$

The electrochromic behaviors, as written in the two reactions above, were observed experimentally. In addition, it was determined from the previous PWECB work [1] that a maximum H^+insertion level (x in H_xWO_3) of *ca.* 0.33 is attained when a potential of -0.5 V (*vs.* Ag/AgCl/sat'd KCl) is applied to the WO_3 electrode immersed in the K-PAMPS electrolyte. Thus, by taking an average of the cathodic and anodic peak potentials, the formal potentials for the InHCF/KInHCF and $WO_3/H_{1/3}WO_3$ redox couples are estimated to be *ca.* 0.867 V and *ca.* -0.372V (*vs.* Ag/AgCl/sat'd KCl), respectively. Accordingly, it is inferred that an IWECB using the K-PAMPS electrolyte possesses a theoretical cell voltage of *ca.* 1.24 V. It's a common practice to take an average value of the cathodic and anodic peak potentials as the formal potential. However, in a more rigorous approach, one needs to consider the transport properties of each diffusional species.

3.1.2 *Redox capacities of the InHCF/KInHCF and WO_3/H_xWO_3 redox couples*

The redox charge capacities for the InHCF and WO_3 films are calculated from the CVs in Fig. 1 to be *ca.* 27.6 mC/cm^2 (=124 mC) and *ca.* 32.4 mC/cm^2 (= 146 mC). It is worthwhile mentioning that the InHCF film, grown in the improved plating solution [1] by the 30-scan CV electrodeposition, has a much larger charge capacity (several-thousand times) than those of the films grown in the unmodified, dilute plating solutions [2-3, 16-17]. Obviously, the InHCF film with a charge capacity of 27.6 mC/cm^2 achieved by the improved InHCF electrodeposition is needed to qualify the film as a workable thin-film electrode. Previously, all known methods [2-6, 16-17] produced films with a much lower charge capacity, and thus disqualify the film as a practical thin-film electrode. With regard to the theoretical capacity for an InHCF electrode, reaction (1) suggests a value of 73.3 mAh/g (based on In[Fe(CN)$_6$]). This value is *ca.* 1.26 times that of the BG/PB redox system and is *ca.* 1.92 times that of the $WO_3/H_{1/3}WO_3$ [1]. However, a practical charge density (mAh/cm^3) consideration gives a reverse order. According to the redox's charge capacities (mC/cm^2) estimated from CVs and the film thickness determined by a profile meter [1], the practical charge densities for the InHCF/KInHCF, BG/PB, and $WO_3/H_{1/3}WO_3$ redox systems are estimated to be 38.5 mAh/cm^3, 46.9 mAh/cm^3, and 200 mAh/cm^3, respectively. When compared with the theoretical charge densities of 150 mAh/cm^3 (InHCF), 112 mAh/cm^3 (PB), and 275 mAh/cm^3 (WO_3), calculated according to the ideal lattice parameters, the relative densities for the InHCF, PB, and WO_3 films are read as *ca.* 0.26, 0.42, and 0.72, respectively. The relative densities could be underestimated due to non-ideal crystalline structures. (In other words, the theoretical charge densities could be overestimated.) Nevertheless, it could be inferred that the post-heated WO_3 film is the most compact, whereas the InHCF film is the least compact.

3.1.3 *Typical charge/discharge characteristics of an IWECB*

It was mentioned in Section 3.1.1 that an IWECB has a theoretical voltage of *ca.* 1.24 V. To verify this theoretical voltage, a typical charge/discharge curve for an IWECB is given in Fig. 2. It shows that an IWECB can be reversibly charged/discharged between 0.70V and 1.70V at a rate of 0.04 mA/cm^2(= 0.18 mA, equivalent to a C-rate of *ca.* 7.7 C). The selection of the charge/discharge rate at 0.04 mA/cm^2 is not totally arbitrary. Notice that the middle point of the corresponding cell voltages at this charge/discharge rate is very close to the theoretical cell voltage. Although it has not been optimized yet, the operation limit of an IWECB, ranging from 0.70V to 1.70V, is adequate. By taking an average of the flattest voltages during the charge and discharge processes, a mean cell voltage of *ca.* 1.15 V, which is slightly lower than 1.24 V, is attained. The difference of 0.09 V is presumably attributed to the non-unity charge capacity ratio [24] between the InHCF and WO_3 films, which should be avoidable. Additionally, since a 1.70 V IWECB is discharged to 0.70 V within *ca.* 447 sec at 0.04 mA/cm^2, the charge capacity of the cell is estimated to be *ca.* 17.9 mC/cm^2 (= 80.6 mC). Accordingly, the energy capacity is estimated to be 20.6 mWs/cm^2 (= 92.6 mWs). Although the electrochemical performances of the IWECB should be dominated by the InHCF electrode, which has a lower charge capacity than that of the WO_3, the calculated cell's discharge capacity (17.9 mC/cm^2) is only *ca.* 65% of the InHCF's charge capacity. This implies that the discharge process, as shown in Fig. 2 and terminated at 0.70 V, is not complete. In contrast to the PWECB reported previously, the IWECB appears to have a less promising electrochemical performance; however, it is still applicable to low-power electronic devices. Moreover, an IWECB offers vivid electrochromism, which is not available in a PWECB. This will help in promoting the utilization of solar energy, which is to be discussed in the next section.

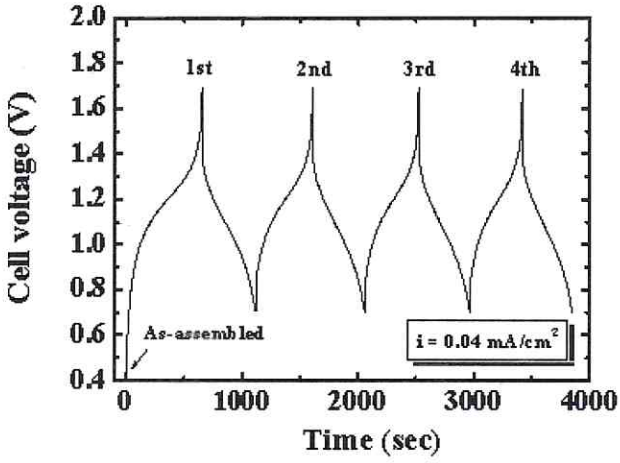

Figure 2: Typical charge/discharge curve for an IWECB. The charge/discharge rate is 0.04 mA/cm^2; the active area of an IWECB is 4.5 cm^2.

3.2 An IWECB with a high visual contrast and its novel applications

3.2.1 *Blue-to-colorless electrochromism of an IWECB*

According to reaction (1) and reaction (2), the overall redox reaction of an IWECB can be written as follows:

$$3WO_3 \text{ (colorless)} + KInHCF \text{ (colorless)} + H^+$$
(The fully discharged state)

$$\leftrightarrow 3H_{1/3}WO_3 \text{ (blue)} + InHCF \text{ (yellowish)} + K^+$$
(The fully charged state) (3)

Eq. (3) indicates that an IWECB is colorless at the fully discharged state but becomes blue upon charging. This implies that an IWECB shows a much higher visual contrast between the charged and discharged states, when compared with the PWECB that exhibits blue-to-dark green electrochromism. This high visual contrast is demonstrated in Fig. 3, where Fig. 3 (a) is a picture of an IWECB switched at a cell voltage of 0.70 V; Fig. 3 (b) is a picture for the same cell switched at 1.70 V. Apparently, the IWECB is superior to the PWECB from the viewpoint of the SOC visualization. To further discuss the electrochromism of an IWECB, the *in situ* transmittive spectra obtained at different equilibrated cell voltages are presented in Fig. 4. Note that this *in situ* experiment was carried out from 0.4 V, which was the cell voltage of an as-assembled IWECB and yielded the most transparent appearance, to 1.7 V in the darkest state.

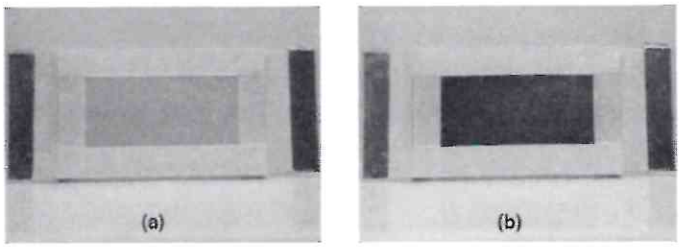

Figure 3: Pictures for an IWECB photographed (a) at 0.70 V, and (b) at 1.70 V.

It is observed in Fig. 4 that the transmittance in the visible spectra for an IWECB decreases as the cell voltage increases. An absorptive band at 410 nm appears when the cell voltage is larger than 0.9 V. This indicates the formation of the yellowish In[Fe(CN)$_6$] [4-6]. Also, the formation of the "blue" tungsten bronze, H_xWO_3[21-23] can be judged by the decrease in the transmittance at 650 nm. To further illustrate the optical outputs in response to the change in the cell voltage, the transmittances at 410 nm and 650 nm in Fig. 4 are picked out and re-plotted in Fig. 5. It is found that the transmittance modulation at 650 nm (50.6 %) is larger than that at 410 nm (28.0 %). (Note that the transmittance of a FTO glass substrate is *ca.* 80%. This implies that the visible transmittance modulations will become 79.1% at 650 nm and 43.8% at 410 nm if the conducting glass substrates with a transmittance of 100 % are used.) As a result, the blue-to-colorless electrochromism is dominant over the yellowish-to-colorless electrochromism. Moreover, it is shown in Fig. 5 that the transmittance at 650 nm decreases drastically beyond 0.8 V during discharging. Since a battery generally fails to drive an electronic device at 0.8 V, this rapid color fading seen at 0.8 V can serve as a warning sign for a shortage of charge. As a consequence, the ECB based on the InHCF and WO_3 electrodes will be a potential system for visualizing the SOC.

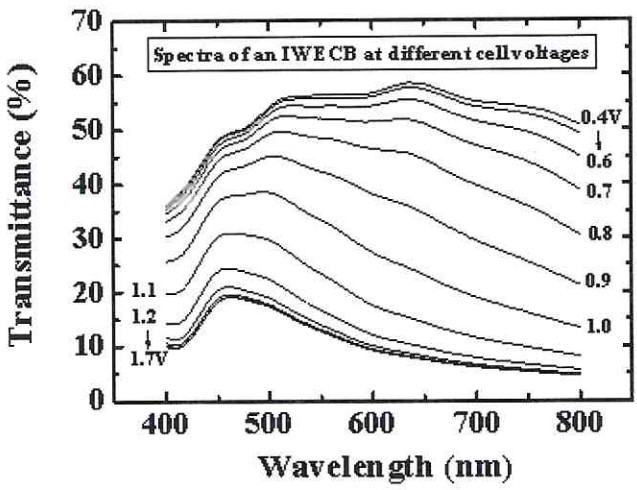

Figure 4: Transmittive spectra for an IWECB measured at different equilibrated cell voltages.

3.2.2 *From the dual energy-saving function to enhancing the utilization of solar energy*

Since an IWECB possesses not only a workable cell voltage but also vivid electrochromism, the dual energy-saving function of the system is to be expected: to act as a rechargeable battery and/or a solar-attenuated window. For applications in a rechargeable battery, it was demonstrated, similar to those presented in the previous PWECB work [1], that an IWECB with an energy capacity of 20.6 mWs/cm^2 (= 92.6 mWs) could drive a low-power electronic device, such as an 8-digit electronic calculator, electronic timer and electronic temperature-humidity indicator, for a few hours. Once again, the promising, combinative PV-IWECB power system has been shown experimentally to be feasible, and will be described later.

On the other hand, for applications of an IWECB in electrochromic windows, as documented by Spindler [11], the following electrochromic properties as well as solar-attenuated properties were investigated and determined. First, the coloration efficiencies [25] of an IWECB at 410 nm and 650 nm are calculated to be 31.7 cm^2/C and 46.0 cm^2/C, respectively. This is based on the transmittances measured at 0.70 V (T_{410nm} = 35.9 %; T_{650nm} = 51.0 %) and at 1.70 V (T_{410nm} = 9.72 %; T_{650nm} = 7.65 %) and the corresponding charge capacity estimated from

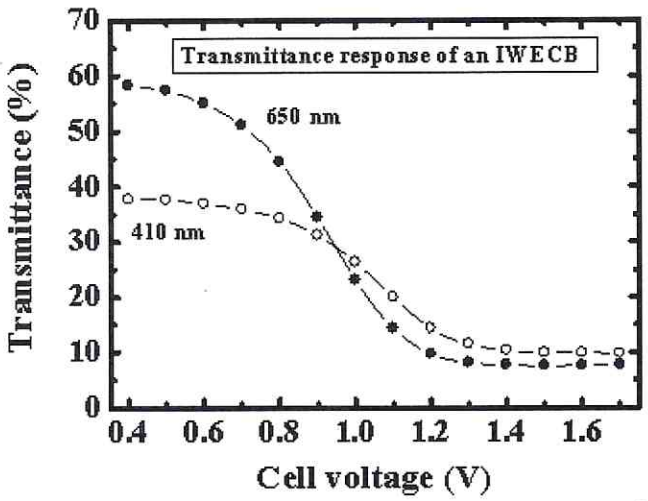

Figure 5: Plots of transmittance *vs.* cell voltage at 410 nm and 650 nm. The data are taken from Fig. 4.

Fig.2 (17.9 mC/cm^2). Second, the integrated transmittance cut-off fraction in the visible range, $\Delta_T(\%)$, which is defined in Eq. (4), is determined from the transmittance spectra modulated between 0.40 V (the as-assembled state) and 1.70 V (the fully charged state).

$$\Delta_T \equiv \frac{\int T_{max}(\lambda)d\lambda - \int T_{min}(\lambda)d\lambda}{\int T_{max}(\lambda)d\lambda} \qquad (4)$$

Where Δ_T is the integrated transmittance cut-off fraction in the visible range, $T_{max}(\lambda)$ and $T_{min}(\lambda)$ represent the most transparent and the darkest transmittive spectrum, respectively, and λ is the wavelength ranged from 400 nm to 800 nm. From Fig. 4, the Δ_T value is calculated to be *ca.* 80.4 %. This means that an IWECB with a large charge capacity ensures that *ca.* 80.4% of the integrated transmittance in the visible range will be cut off after complete coloration. This well serves as a solar-attenuated window even though the coloration efficiency is relatively low as compared to that of the complementary PB-WO_3 ECD [26]. As a consequence, an IWECB with a dual energy-saving function can greatly promote the utilization of solar energy.

The corresponding applications of an IWECB are illustrated schematically in Fig. 6. Fig. 6 (a) illustrates the daytime application of an IWECB-based window. Combined with a PV cell, the IWECB window charged by an illuminated PV cell not only stored the solar energy but also colored to attenuate the solar irradiation. Yet the nighttime application, as illustrated in Fig. 6 (b), is a reverse process of the daytime operation. The dark and charged IWECB window can be bleached to increase the interior illumination by discharging and to drive low-power electronic devices after sunset. As can be seen in Fig. 6 (a) and Fig. 6 (b) better utilization of the solar energy has been achieved through incorporating an IWECB with a high visual contrast into a PV cell.

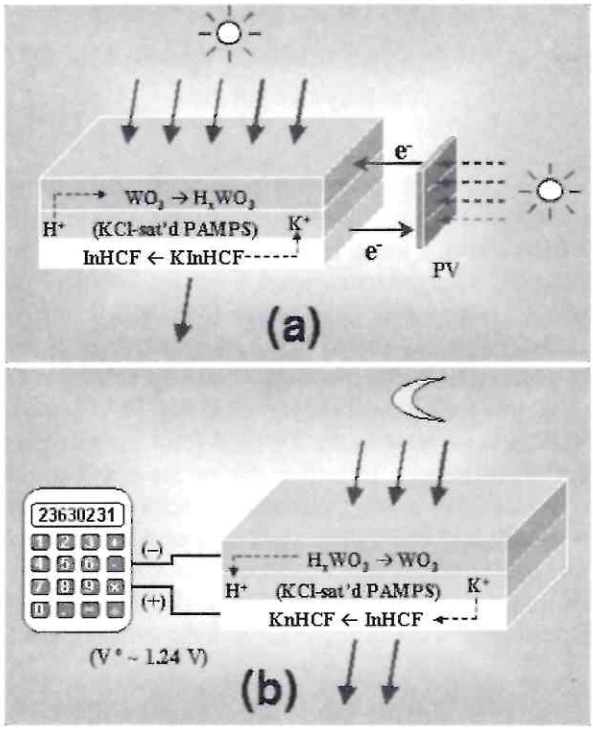

Figure 6: (a) The daytime application of an IWECB-based window (to store the solar energy and to attenuate the solar irradiation); (b) the nighttime application of an IWECB-based window (to drive low-power electronic devices and to increase the interior illumination).

3.3 Dynamic and at-rest stabilities of an IWECB

After describing the principle and attractive applications of an IWECB, the experimental results of dynamic and at-rest stabilities are to be presented and discussed in this section.

3.3.1 Dynamic stability of an IWECB: cycle life

Fig. 7 describes the cycling characteristics of a fresh IWECB, which was charged/discharged between 0.70V and 1.70V 1,000 times by applying a constant current density of 0.1 mA/cm^2 (0.45 mA). The discharge time for the 1^{st} cycle is 55.9 s. In this figure, two indices η_n and θ_n, as defined in the previous work [1], are plotted to evaluate the dynamic stability, where η_n denotes the ratio of the n^{th} discharge capacity to the n^{th} charge capacity (the discharge-to-charge efficiency of the n^{th} cycle); θ_n represents the discharge capacity ratio of the n^{th} cycle to that of the 1^{st} cycle. It is shown that η_n, with an initial value of *ca.* 45 %, increases rapidly in the first 10 cycles to *ca.* 97%

and then approaches 100% after the 25^{th} cycle. Concerning θ_n, it cannot be considered as an index to evaluate the cycling loss in discharge capacity here, although such a consideration was valid for a PWECB [1]. It is observed in Fig. 7 that θ_n first increases to a value of *ca.*144% at the 25^{th} cycle but then gradually decreases to a value of *ca.* 48.5% at the $1{,}000^{th}$ cycle. In addition, θ_n is greater than 100% for the first 300 cycles. The cycling gain in the first 300 cycles, rather than the cycling loss, is probably due to the incomplete discharge, which was pointed out in Section 3.1.3. That is, the IWECB discharged to 0.70V at a high current rate of 0.45 mA may still contain some residual capacity, which must be released and counted in the subsequent discharge cycles; therefore, a cycling gain, instead of a cycling loss, was observed. In fact, it was observed experimentally that the discharging process of an IWECB is slower than the charging process from the viewpoint of kinetics, and the slower reduction process of InHCF is responsible for this observation. (Refer to Fig. 1, where the anodic peak of the InHCF's CV is sharper than the cathodic peak.) To improve the unstable cycling property, a complete and slow discharging of an IWECB is required. With respect to the decrease in the discharge capacity observed after several hundred cycles, presumably, that is due to the gradual dissociation of In[Fe(CN)$_6$] to form In^{3+} and $[Fe(CN)_6]^{3-}$ at the high charging voltages. Similar to the case of a PWECB, this argument is deduced from the 100% discharge-to-charge efficiency (η_n). Of course, lowering the upper boundary of the charging voltage and shortening the duration at which the unfavorable high voltages are being applied should solve the problem of the dissociation. Additionally, it is noticed that using a Ru-modified InHCF, as suggested by De Benedetto *et al.* [16] and Cataldi *et al.* [17], a better cycle life may be achieved.

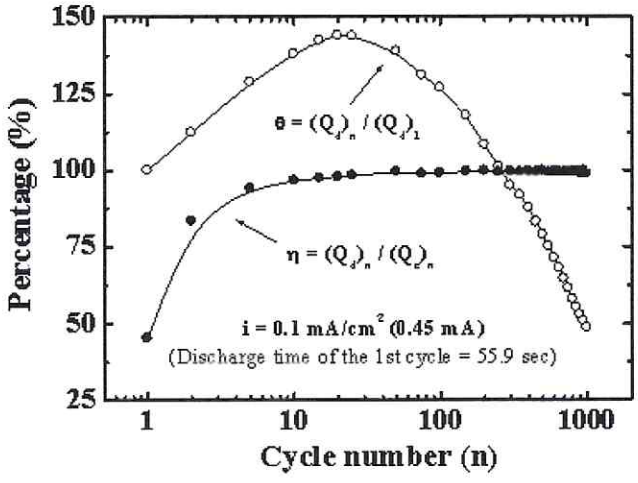

Figure 7: The dynamic stability test for a fresh IWECB, which is charged/discharged between 0.70V and 1.70V 1,000 times by applying a constant current of 0.45 mA.

3.3.2 *At-rest stability of an IWECB: self-discharging rate*

Fig. 8 compares the self-discharging with a typical discharging at a rate of 0.04 mA/cm^2 for a fresh IWECB. Accordingly, a self-discharging rate of *ca.* 0.12 μA/cm^2 is estimated. This self-discharging rate is almost a third that of a fresh PWECB and means that it will take *ca.* 8,333 hours (347 days, almost 1 year) to completely self-discharge an IWECB with a charge capacity of 1 mAh/cm^2, as long as a good sealing condition is ensured! Obviously, this is another unique characteristic of an IWECB. Regarding the smaller self-discharging rate as compared to that of a PWECB, the self-discharging mechanism, as suggested below, is proposed. The self-discharging of a fully charged IWECB (InHCF/K-PAMPS/$H_{1/3}WO_3$) is attributed to the presence of H_2O and O_2 in the K-PAMPS electrolyte [1] as in the case of PWECB. The related mechanisms may be written as follows.

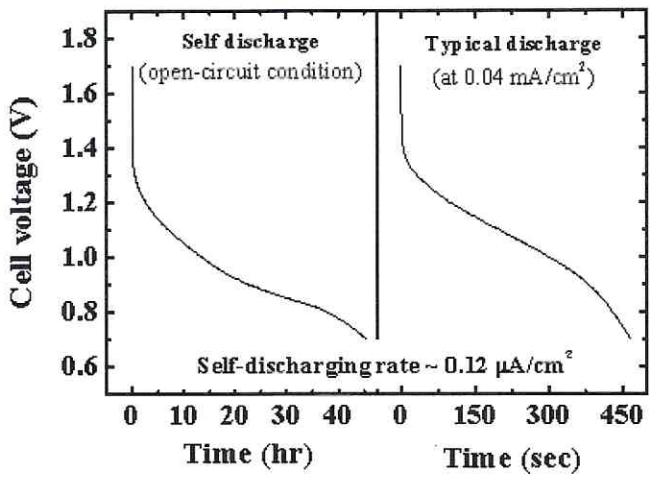

Figure 8: Comparison between the self-discharging and typical discharging for a fresh IWECB. Before performing these experiments, the IWECB was charged at a rate of 0.04 mA/cm^2 to 1.70V.

Positive electrode: $$In[Fe(CN)_6] + 1/2H_2O + K^+ \rightarrow KIn[Fe(CN)_6] + 1/4O_2 + H^+ \quad (5)$$

Negative electrode: $$H_{1/3}WO_3 + 1/12O_2 \rightarrow WO_3 + 1/6H_2O \quad (6)$$

Reaction (5) describes the chemical reduction of InHCF in the presence of H_2O to form KInHCF; reaction (6) elucidates the

chemical oxidation of H_xWO_3 in the presence of oxygen. According to the standard potential for the electro-hydrolysis process in the presence of H^+ [27] and the formal potentials for the InHCF/KInHCF and WO_3/H_xWO_3 redox couples, the standard Gibbs free energy (ΔG^o at 25°C) for the above two reactions is estimated to be 15.92 kJ/mole InHCF and -33.90 kJ/mole $H_{1/3}WO_3$, respectively. In contrast to the free energy for the chemical reduction of BG in the presence of H_2O (3.73 kJ/mole BG), InHCF has a more positive value (4.27 times); therefore, InHCF is more difficult to reduce chemically than BG. Additionally, the driving force of the self-discharging process for an IWECB is predominately determined by the chemical oxidation of $H_{1/3}WO_3$ with oxygen; hence, a self-discharging process, which proceeds at a much slower rate, shows a lower mid-point voltage (MPV) than that of a typical discharge (see Fig. 8).

4. CONCLUSION

Under the improved InHCF plating conditions, an IWECB in combination with a K-PAMPS electrolyte, which accommodates the conduction of both K^+ and H^+, has been investigated. Moreover, applicability of an IWECB has been demonstrated. In addition to having the advantages outlined in the previous PWECB work, an IWECB with a high visual contrast shows superiority in the visualization of the SOC and in the utilization of solar energy although the theoretical voltage of an IWECB is lower than that of a PWECB by 0.11V. To conclude this work, some pivotal findings for an IWECB are summarized as follows.

1. *Workable cell voltage*: An IWECB can be charged/discharged between 0.70 V and 1.70 V. The cell provides a theoretical voltage of 1.24 V and is capable of driving a low-power electronic device.

2. *High visual contrast*: An IWECB exhibits blue-to-colorless electrochromism during the discharging process. Therefore, it offers better SOC visualization than that of a PWECB.

3. *High electrochemical reversibility*: The 100% discharge-to-charge efficiency can be attained within few charge/discharge cycles (says, 25 cycles) and kept constant for more than 1,000 cycles. Apparently, the electrochemical reversibility is also affected by the charge/discharge rate and the corresponding voltage ranges.

4. *Unique dynamic characteristics*: A cycling gain instead of a cycling loss was recorded for the first 300 cycles in a 1,000-time charge/discharge cycling test. Presumably, it could be attributed to the incomplete discharging of an IWECB. The long-term cycling loss can be improved by shortening the duration at which the high voltages are being applied to prevent the dissociation of $In[Fe(CN)_6]$.

5. *Good at-rest stability*: The estimated self-discharging rate for an IWECB is about 0.12 $\mu A/cm^2$, which is almost a third that of a PWECB. Under a perfect sealing condition, this means that it will take almost a year to completely self-discharge an IWECB with a capacity of 1 mAh/cm^2.

6. *Dual energy-saving function*: Besides functioning as a rechargeable battery to drive a low-power electronic device, an IWECB with a high visual contrast can act as a solar-attenuated window. Although the electrochromic window based on an IWECB only has a coloration efficiency of *ca.* 46 cm^2/C at 650 nm, the large cell charge capacity of 17.9 mC/cm^2 promises that 80.4% of the integrated transmittance in the visible range will be cut off upon complete coloration.

7. *Promoting the use of solar energy*: When an electrochromic window based on the IWECB is charged by a PV cell to store solar energy in the daytime, it will be colored correspondingly, and thus attenuate the solar irradiation. On the contrary, the reverse process can be performed to provide the DC charge and to enhance the illumination at night.

According to the above findings, an IWECB with multiple functions, in addition to its standard use as a rechargeable battery or an ECD, can serve as a superior electro-optical device and promises better utilization of solar energy.

5. ACKNOWLEDGMENTS

The authors wish to thank Sinonar Corporation, Hsinchu, Taiwan, for providing the conductive FTO-coated glass substrates. This research was supported by the National Research Council of the Republic of China under Grant NSC 89-2214-E002-072.

REFERENCES

[1] L.-C. Chen, Y.-H. Huang, K.-S. Tseng, and K.-C. Ho, *J. New Mater. Electrochem. Systems*, **5**, **VOIRPAGE** (2002)

[2] P. J. Kulesza and M. Faszynska, *J. Electroanal. Chem.*, **252**, 461 (1988).

[3] P. J. Kulesza and M. Faszynska, *Electrochim. Acta*, **34**, 1749 (1989).

[4] S. Dong and Z. Jin, *Electrochim. Acta*, **34**, 963 (1989).

[5] M. A. Malik, G. Horanyi, P. J. Kulesza, G. Inzelt, V. Kertesz, R. Schmidt, and E. Czirok, *J. Electroanal. Chem.*, **452**, 57 (1998).

[6] K. C. Ho and J. C. Chen, *J. Electrochem. Soc.*, **145**, 2334 (1998).

[7] K. Itaya, I. Uchida, and V. D. Neff, *Acc. Chem. Res.*, **19**, 162 (1986).

[8] R. J. Mortimer and D. R. Rosseinsky, *J. Electroanal. Chem.*, **151**, 133 (1983).

[9] H. J. Buser, D. Schwarzenbach, W. Petter, and A. Ludi, *Inorg. Chem.*, **16**, 2704 (1977).

[10] F. Herren, P. Fischer, A. Ludi, and W. Hälg, *Inorg. Chem.*, **19**, 956 (1980).

[11] R. Spindler, *U. S. Pat.*, 5, 209, 980 (1993).

[12] L.-C. Chen, Y.-H. Huang, and K.-C. Ho, in "Proceeding of the Advanced Batteries and Accumulators", Eds., J. Vondrák and M. Sedlaříková, Technical University of Brno, Brno, Czech Republic (2001), **Vol. II**, p. 11-1.

[13] S. Zhang, W.-L. Sun, W. Zhang, W. Y. Qi, L. Y. Jin, K. Yamamoto, S. Tao, and J. Jin, *Analytica Chimica Acta*, **386**, 21 (1999).

[14] L.-C. Chen, Y.-C. Hsu, and K.-C. Ho, in "Meeting Abstracts", 2001 Joint International Meeting of the Electrochemical Society and the International Society of Electrochemistry, 2001, **Vol. 2001-2**, Abstract No. 1078.

[15] T. Gruszecki and B. Holmstrom, *J. Appl. Electrochem.*, **21**, 430 (1991).

[16] G. E. De Benedetto and T. R. I. Cataldi, *Langmuir*, **14**, 6274 (1988).

[17] T. R. I. Cataldi and G. E. De Benedetto, *J. Electroanal. Chem.*, **458**, 149 (1998).

[18] E. W. Grabner and S. Kalwellis-Mohn, *J. Appl. Electrochem.*, **17**, 653 (1987).

[19] M. Jayalakshmi and F. Scholz, *J. Power Sources*, **91**, 217 (2000).

[20] L.-C. Chen, K.-S. Tseng, and K.-C. Ho, in "Proceeding of the Advanced Batteries and Accumulators", Eds., J. Vondrák and M. Sedlaříková , Technical University of Brno, Brno, Czech Republic (2001), **Vol. II**, p. 10-1.

[21] S. K. Deb, *Appl. Opt. Suppl.*, **3**, 193 (1969).

[22] R. S. Crandall, P. J. Wojtowicz, and B. W. Faughnan, *Solid State Commun.*, **18**, 1409 (1976).

[23] C. G. Granqvist, *Solar Energy Mater. & Solar Cells*, **60**, 201 (2000).

[24] L.-C. Chen and K.-C. Ho, *Electrochim. Acta*, **46**, 2159 (2001).

[25] P. M. S. Monk, R. J. Mortimer, and D. R. Rosseinsky, *Electrochromism: Fundamentals and Applications*, VCH, Weinheim, Germany (1995): Section 1.4.3.

[26] K.-C. Ho, T. G. Rukavina, and C. B. Greenberg, *J. Electrochem. Soc.*, **141**, 2061 (1994).

[27] A. J. Bard and L. R. Faulkner, *Electrochemical Methods: Fundamentals and Applications*, 2^{nd} ed., John Wiley & Sons, USA (2001): Table C.1 in Appendix C.